Effects of Permeability on the Dynamic Properties and Weathertightness of Double Skin Curtain Walls

Kehinde J. Alawode, A.M.ASCE[1]; Krishna Sai Vutukuru, S.M.ASCE[2]; Amal Elawady, Ph.D.[3]; Seung Jae Lee, Ph.D.[4]; Arindam Gan Chowdhury, Ph.D.[5]; and Guido Lori, Ph.D.[6]

[1]Dept. of Civil and Environmental Engineering, Florida International Univ., Miami, FL. Email: kalaw003@fiu.edu
[2]Dept. of Civil and Environmental Engineering, Florida International Univ., Miami, FL. Email: kvutu001@fiu.edu
[3]Dept. of Civil and Environmental Engineering, Extreme Events Institute, International Hurricane Research Center, Florida International Univ., Miami, FL. Email: aelawady@fiu.edu
[4]Dept. of Civil and Environmental Engineering, Florida International Univ., Miami, FL. Email: sjlee@fiu.edu
[5]Dept. of Civil and Environmental Engineering, Extreme Events Institute, International Hurricane Research Center, Florida International Univ., Miami, FL. Email: chowdhur@fiu.edu
[6]Group Innovation and Technology, Permasteelisa S.p.A, Vittorio Veneto, Treviso, Italy. Email: g.lori@permasteelisagroup.com

ABSTRACT

Cavity permeability influences the rate of pressure equalization and load sharing between the two glazed walls of a double skin curtain wall. It is also known to affect weathertightness in these non-structural systems. However, in testing the weathertightness of curtain wall systems, manufacturers and regulators usually use testing sequences that do not replicate realistic wind events or co-occurring wind and rain events, which are some of the factors leading to water penetration and mist formation within the cavity of double skin systems. A full-scale wind testing study was carried out on a novel closed cavity double skin glazed curtain wall unit at 22.4 m/s, 31.3 m/s, and 40.2 m/s wind speeds with wind directions varying between 0° and 360° in 15° increments. This study finds the strong dependence between permeability and load sharing, water penetration, and dynamic properties. It also shows the limit of current code guidance in predicting load sharing at higher permeability.

Keywords: Pressure equalization, Double skin curtain wall, Wind-Driven Rain, Permeability, Weathertightness, Wind load, Wind-induced vibration

INTRODUCTION

Buildings account for 41% of energy use in the US, with heating, ventilation and air-conditioning (HVAC) systems contributing 50% of this energy usage (USDOE, 2011; Wu et al., 2016). Properly designed double skin glazed curtain walls typically have higher energy efficiency (Fang, et. al, 2020) for maintaining indoor temperature while providing better weathertightness and higher stiffness in comparison to the common single skin facades. Therefore, the double skin units are becoming increasingly popular with the high performance.

External walls in glazed curtain walls can be either face-sealed or water-managed (Van Linden and Van Den Bossche, 2021) or pressure equalized (Killip and Cheetham, 1984). These

systems are designed to resist the factors that drive water penetration, which are; gravity, capillary action, surface tension, kinetic energy, air currents, and pressure difference (Garden, 1963). Face-sealed curtain walls rely on perfect seals between the glass and the frames while water-managed curtain walls rely on the drains within the frames. Pressure equalized curtain walls are usually double skin walls designed based on the pressure equalization theory. The theory is based on the knowledge that differential pressure forces water through gaps and joints between components, and the reduction of this differential pressure would lead to a waterproof system (Killip and Cheetham, 1984). The theory has continued to be improved since the 1960s to understand the parameters affecting the design (Kala, Stathopoulos, and Suresh Kumar, 2008). The closed cavity double skin system combines the pressure equalized and face-sealed design criteria. The cavity in this system has a relatively low permeability in comparison to the pressure equalized system with full face-sealed all around. The permeability of the double skin facades adopting only the PER design criteria can be changed depending on its design requirements (i.e., load sharing, water penetration resistance etc.). Figure 1 shows the traditional PER double skin and the closed cavity double skin system.

Double skin glazed curtain walls have typically shown improved performance in resisting water and air penetration. The principal parts of a typical double skin system are an external wall (rain screen), an air gap (cavity) which is vented to the external/internal, and an internal wall (air barrier). It is important to note that with PER systems, the air gap is usually vented to the external side, whereas the close cavity system can be vented either way. The efficiency of a PER wall depends on how close the external pressures and the cavity pressures are, where the most efficient have a zero pressure difference (Baskaran and Brown, 1992). Matthews et al., (1996) suggest that dynamic water penetration tests are necessary to assess the performance of PER systems; the authors were referring to the procedure in (AAMA 501.1-05, 2005) where a constant water spray and an airplane engine is used as a wind force generator during water penetration tests. However, this water spray and airplane engine produced winds used by manufacturers and regulators do not replicate realistic wind events or co-occurring wind and rain events as shown by previous experiments conducted on residential windows (Vutukuru et al., 2020).

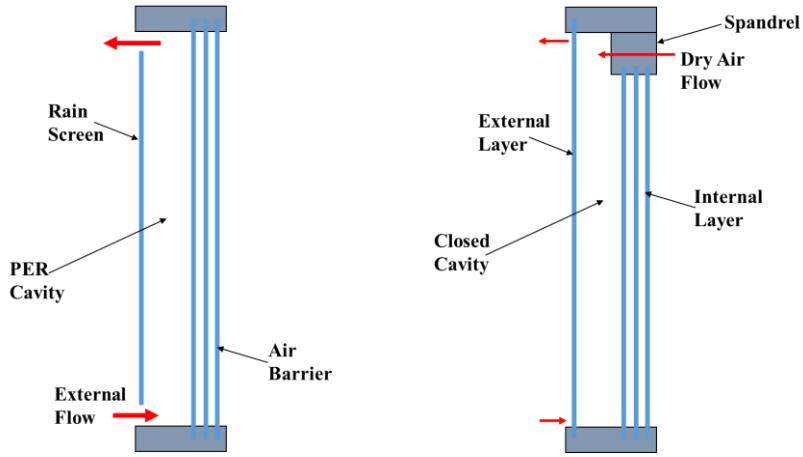

(a) Pressure equalized system (b) Closed Cavity

Figure 1. Schematics of double skin curtain wall (Courtesy of WOW Research Team)

Besides the reduction of water penetration, double skin curtain wall systems share wind loads between the external wall and internal wall (Kumar, 2000). This is also expected with closed cavity systems. Irwin et al., (1984) suggested that the rainscreen can be designed for 70% of the typical wind cladding load if the air gap is well vented and compartmentalized. Ganguli and Dalgliesh (1988) suggest a 75% wind loading for the rainscreen design based on a field study they conducted. However, there are no known suggestions for the closed cavity system as this system is neither fully closed nor well ventilated. Permeability of the double skin system is related to the area of the vents in the external wall/airgap and leakage in the internal wall. The theoretical air tightness of the internal wall might not be usually applicable in the field because manufactured units are not perfectly airtight and degradation of seals over time. Also, these previous studies did not consider the wind induced vibration effects due to the openings in the units.

While double skin curtain walls with pressure equalized systems have received some attention, closed cavity systems have not, as it is relatively new. Most studies on the closed cavity system have focused on its energy efficiency and condensation assessment while its structural performance and optimization have not been systematically tested under realistic wind and rain. Also, the load sharing between the two walls has not been investigated using full-scale wind tunnel tests previously and neither is there a standard to guide designers about load sharing in closed cavity double skin units. To address this knowledge gap, this study conducts full-scale tests on a closed cavity double skin curtain wall unit focusing on the weathertightness and dynamic properties as it relates to the permeability of the cavity. Section 2 describes the experimental methodology; Section 3 discusses the results, and the conclusions are in Section 4.

EXPERIMENTAL SETUP AND DATA ANALYSIS METHOD

The experimental tests were performed at the NHERI Wall of Wind (WOW) experimental facility (EF) at Florida International University. The facility is an open jet wind tunnel capable of producing up to Category 5 hurricane wind speeds of ~70 m/s (Gan Chowdhury et al., 2017).

Model Configuration

The built-up model is supported on a steel structure bolted to the WOW turntable with a rectangular shape of 3 m (width) × 1.83 m (breadth) × 3.65 m (height) and a flat roof with overhangs. Two closed cavity double skin curtain wall units, each measuring 1.35 m (53”) width and 3.63 m (143”) height, were mounted side by side on one of the 3m width sides as shown in Figure 2(a). A polycarbonate side with a geometrically similar arrangement to the curtain walls was attached to a wood frame and placed on the other side as shown in Figure 2(b).

This polycarbonate side allows for the placement of pressure taps to measure external wind pressure because it is impractical to drill the actual glass curtain wall. This would only allow a comparison of net pressures and load sharing ratios in terms of global indices and not by a step by step comparison on the pressure time histories. Figure 3 shows the schematics of the model plan, wind direction and a corner section of the curtain wall unit.

Two configurations of the model were tested, one with ‘closed cavity’ and the other with ‘vented cavity’ (vented cavity is used in this text only to refer to this setup) where a 10 mm diameter opening was created on the side of the unit at the laboratory (shown in figure 4) to represent a possible cavity defect scenario. The external wall is double-glazed while the internal wall is triple glazed. The curtain wall has a cavity depth of 140 mm.

(a) The Glazed side of the model (b) The polycarbonate side of the model

Figure 2. Double skin curtain wall model (Courtesy of WOW Research Team)

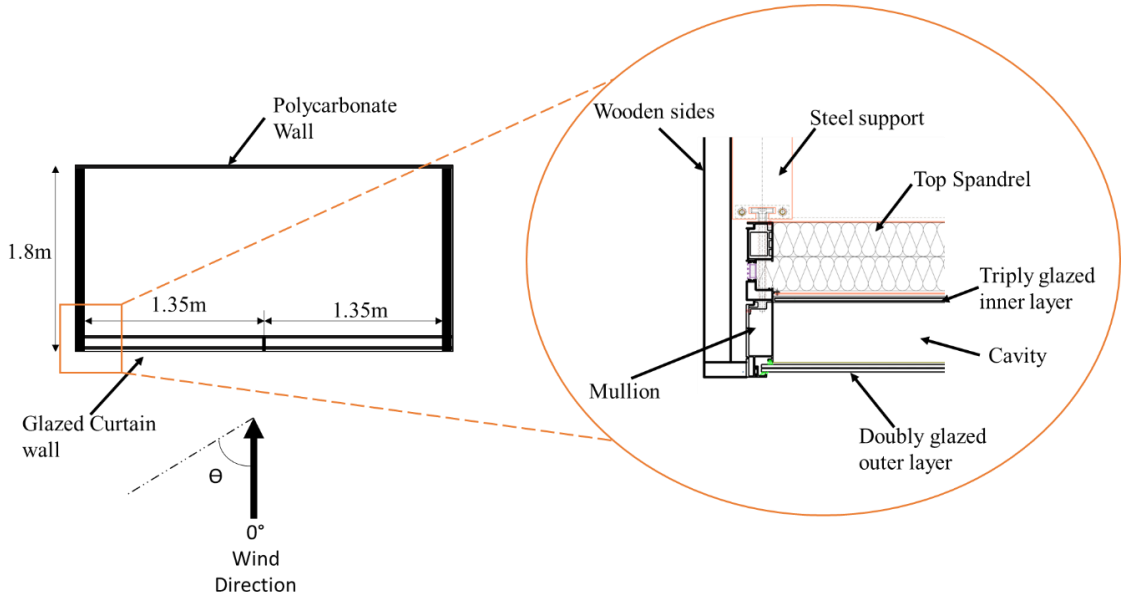

Figure 3. Plan of double skin curtain wall model (Courtesy of WOW Research Team)

Testing Protocol and Instrumentation

An open terrain atmospheric boundary wall (ABL) wind profile was experimentally simulated. Figure 5 shows the wind spectrum, vertical wind speed profile and turbulence characteristic during the simulation at the center of the turntable. The spectrum plot shows a mismatch with ESDU data at lower frequencies. This is accounted for analytically using the partial turbulence simulation (PTS) method (Mooneghi et al., 2016, Moravej, M., 2018).

Figure 4. Vented Cavity DSF (Courtesy of WOW Research Team)

A total of 100 pressure taps were installed on the two polycarbonate walls, one pressure tap in each cavity of the double skin façade unit and two pressure taps within the model building. Figure 6 shows the pressure tap layout where black dots represent the location of the pressure taps. Thermocouples were also placed within the cavity of the curtain wall unit. Accelerometers and strain gauges were attached to the unit (glass and mullion) as shown in Figure 7.

External (on polycarbonate side), cavity (within the double skin units) and internal (inside the steel frame) wind pressure time histories are collected during the tests. The pressure tests were conducted for three wind speeds of 22.35m/s (50mph), 31.3m/s (70mph) and 40.23m/s (90mph), from 0° to 180°, with an increment of 15°, at a 2-minute duration per wind direction. These tests were conducted on both closed cavity and vented cavity configurations.

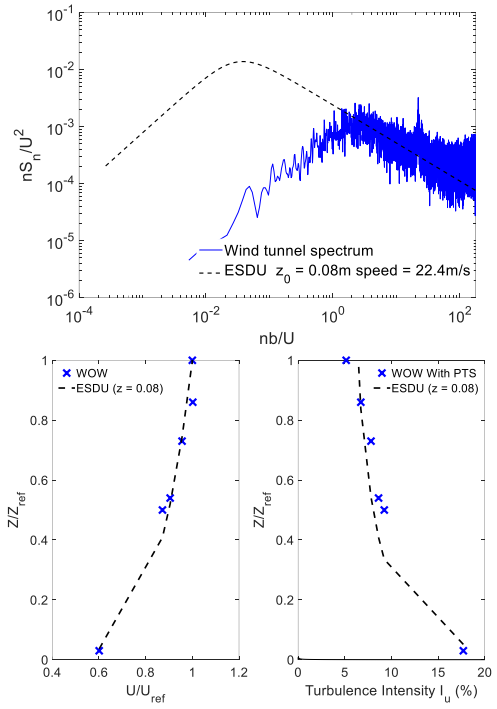

Figure 5. Wind spectrum and vertical wind profile at WOW compared with ESDU (Adapted from ESDU, 2001 and Courtesy of WOW Research Team)

Furthermore, dynamic tests were conducted whereby strain and acceleration time histories were collected. These tests were conducted on the glazed curtain wall side of the specimen at 22.35m/s (50mph), 31.3m/s (70mph) and 40.23m/s (90mph), for wind directions between 0^0 to 180^0 with an increment of 15^0 (see Figure 5b). It is worth noting that the tests were only performed for 0^0 to 180^0 utilizing the geometric and instrumentation symmetry.

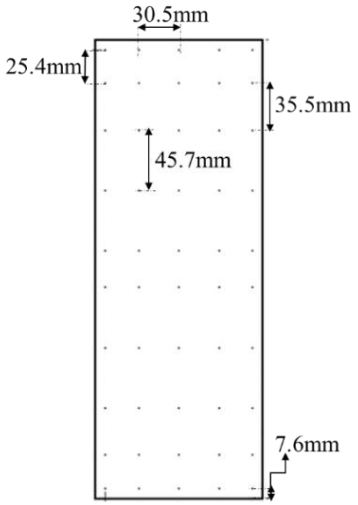

Figure 6. Pressure tap layout on one of the polycarbonate units (Courtesy of WOW Research Team)

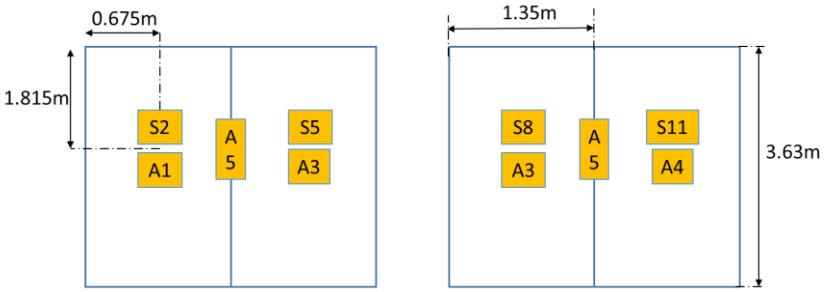

(a) External wall (b) Internal wall

Figure 7. Layout of accelerometers (A) and strain gauges (S) on the double-glazed glass unit (Courtesy of WOW Research Team)

A full-scale (1:1) raindrop size test was developed in the WOW EF. To ensure accuracy and to replicate realistic hurricane rain characteristics, a gamma model developed using rain data for three real hurricanes of Alex, Charley and Gaston by Tokay et al. (2008) is utilized as a base model to match rain characteristics. To obtain the correct Raindrop Size Distribution, 3-D printed nozzles were installed in front of the WOW fans. The wind driven rain (WDR) tests were carried out for both model configurations at 22.35 m/s, 31.30 m/s and 40.23 m/s wind speeds as shown in Table 1. Figure 8 shows the gamma curve for the selected configuration. Water absorbing mats were attached to the building model to measure the water intrusion through the curtain wall by using weight differentials. Details of the protocol are shown in Table 1.

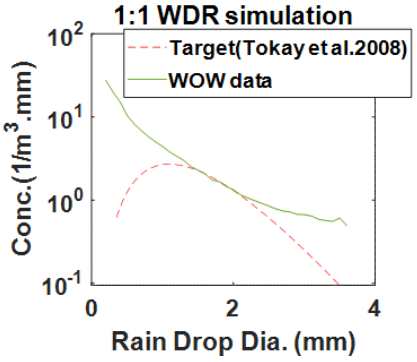

Figure 8. Result fitting gamma curve (Courtesy of WOW Research Team)

Table 1. Testing protocol per configuration

Test Type	Wind Speed (m/s)	Wind Direction (degree)	Test Duration (mins.)
Pressure	22.4, 31.3 and 40.2	0 to 360 in 15 increments	2
Kinetic	22.4	0 to 360 in 15 increments	10
Kinetic	31.3	0 to 360 in 15 increments	5
Kinetic	40.2	0 to 360 in 15 increments	5
WDR	22.4	0, 15, 345	20
WDR	31.3	0, 15, 345	15
WDR	40.2	0, 15, 345	15

Data Analysis

The peak pressure coefficient values are defined by Eq. 1, while Eq. 3 defines the differential cavity pressure:

$$C_{P_{peak}} = \frac{P_{peak}}{\frac{1}{2}\rho U_{3s}^2} \quad (1)$$

$$P_{diff.cav} = P_{cav} - P_{atm} \quad (2)$$

Where, U_{3s} is the peak 3s wind speeds at the roof height of the model, ρ is the air density while P_{peak} is the differential peak pressures, $P_{diff.cav}$ is the differential cavity pressure, P_{cav} is the cavity pressure and P_{atm} is the atmospheric pressure. Before finding the value of pressure coefficients, a suitable tubing transfer function is applied to correct for distortions due to tubing length. The peak Cp values were estimated and corrected analytically using the partial turbulence simulation (PTS) method mentioned earlier.

RESULTS AND DISCUSSION

Pressures

Figure 9 shows the $C_{P_{peak}}$ plot on the curtain wall surface from a wind direction of 0° (i.e., wind perpendicular to glazing). The pattern and values correspond to expected Cp patterns on a

wall. Figure 10a shows a schematic of the wind flow at 0° wind direction with the accompanying cavity differential pressure shown in Figure 10b. The figure shows that the cavity pressure increases with wind speed in the closed cavity configuration. However, suction pressures are observed in the vented cavity configuration at 22.4 m/s and 31.3 m/s. This is due to the cavity being in contact with an external environment (through the 10mm hole) under suction wind pressures as indicated in Figure 10a. At 40.2 m/s a mildly positive pressure is observed indicating the dependence of the cavity pressure on wind speeds in the vented cavity case. Observation of the time series of differential internal pressure within the model and the differential cavity pressure for the vented cavity configuration shows an equalization of the two (i.e., internal environment and cavity) at 31.3m/s and 40.2m/s. This equalization was not observed at 22.4m/s and it best explains the difference in the plot shown in Figure 10b.

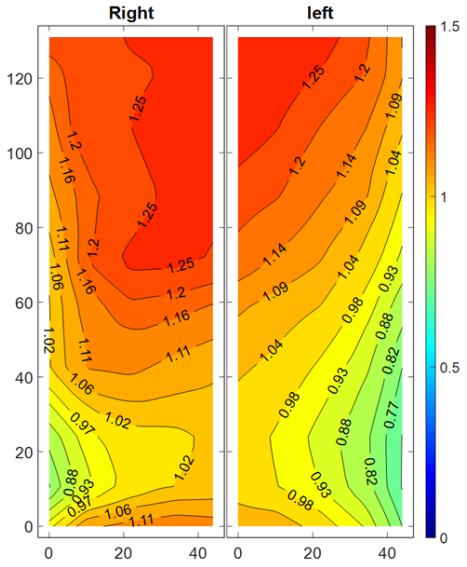

Figure 9. $C_{P_{peak}}$ for curtain wall at 0° and 22.4 m/s (Courtesy of WOW Research Team)

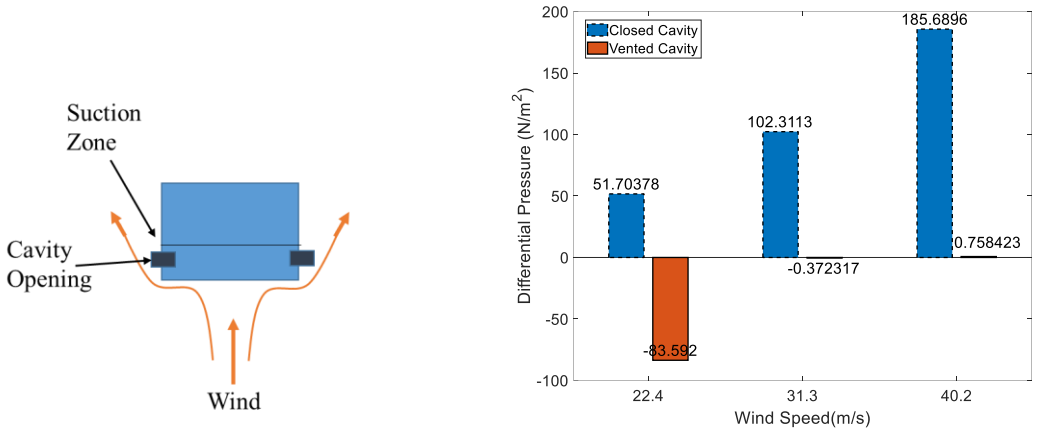

Figure 10 Differential cavity pressure at 0°: (a) Schematic wind flow; (b) Differential cavity pressure comparison between closed and vented cavities. (Courtesy of WOW Research Team)

Accelerations

The acceleration root mean square (RMS) comparison for both configurations is shown in Figure 11. As expected, the accelerations increase with the increasing wind speed. In general, the vented cavity configuration tends to be more susceptible to vibration. However, contrary to the expected result, at low wind speed (22.4m/s), for the internal glass wall, the vented cavity specimen has a lower RMS value compared to the closed cavity. This phenomenon can be attributed to the significant negative cavity pressure for this case as seen in Figure 10b. This makes a case for the sufficiency of quality control in areas experiencing lower wind speeds for the defect case considered and wind direction. However, at higher wind speeds especially at tropical storm range wind speeds, quality control becomes important for sustainable curtainwall design as can be seen from these results. This difference in the performance of vented cavity units based on wind speed needs further investigation.

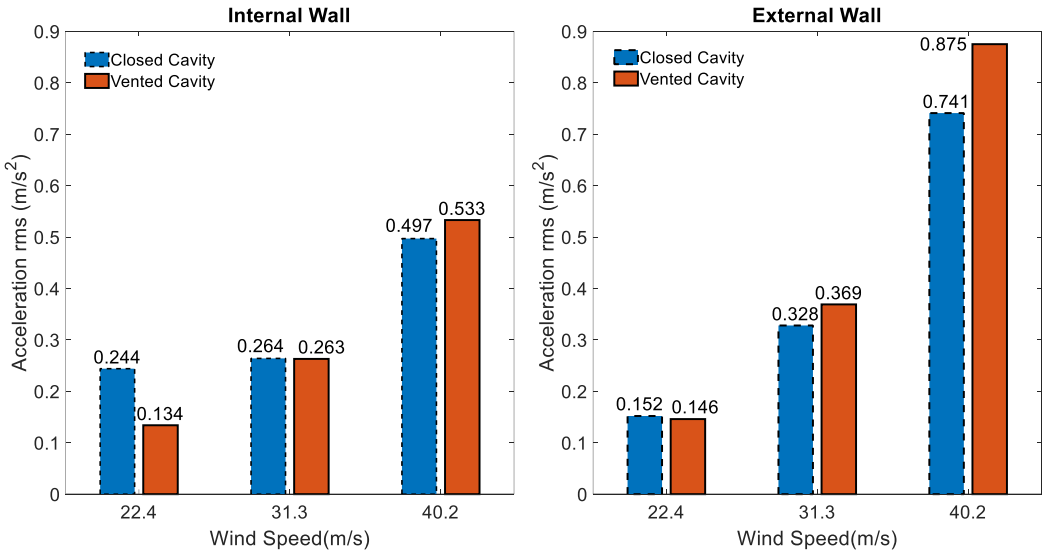

Figure 11. Acceleration RMS at 0° wind direction (Courtesy of WOW Research Team)

Strains

The mean strains on the central mullion, center of external and internal glass wall at 0° wind direction, are shown in Figure 12. The plot indicates an increase in strain with increasing wind speeds for the mullion and external glass in both configurations. The influence of permeability is negligible on the mullions, given the close values of strains in both configurations. This is expected, as the mullion strains are dependent on the total net pressure through the curtain wall. However, permeability influences the strains observed on the glazing, with higher strains observed on the external glass in the vented cavity configuration. The opposite is observed for the internal glass wall, where higher strains are observed on the internal glass of the closed cavity configuration. The lower strain value observed at 40.2m/s relative to 31.3m/s in the internal glass wall of the vented cavity results from the reversal of cavity pressure as shown in Figure 10b. It indicates the dependence of the glass strain on cavity pressure which is in turn dependent on wind speed, highlighted in the discussion on differential cavity pressure results.

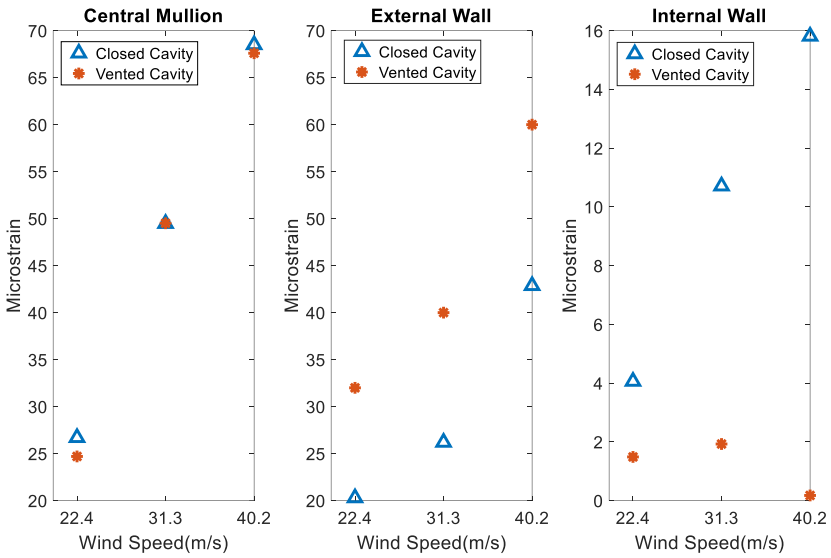

Figure 12. Mean central strains on central mullion, external and internal glass at 0° wind direction (Courtesy of WOW Research Team)

Load Sharing

Load sharing between the external and internal glazing wall in the double skin curtain wall was calculated as the ratio of cavity pressure to external pressure given in Eq. 3. It was observed that the load sharing is mainly driven by the stiffness of each wall for the closed cavity configuration. Table 2 shows a comparison of load sharing ratio (LSR) in the closed cavity and vented cavity configuration in comparison with the value recommended by EN 16612 (2017) for the equivalent system. It is important to note that EN 16612 (2017) is specifically for insulating glazing units (IGU) with cavity depths around 20mm. The load sharing ratios in the closed cavity configuration were like those predicted by EN 16612 (2017) for IGU. However, for the vented cavity configuration, load sharing is driven by a combination of permeability and stiffness which cannot be predicted using the EN 16612 (2017) guidelines. For the tested case, the vented cavity configuration indicates that more than 98% of the wind loads are on the external wall.

$$LSR = \frac{Mean\ (P_{diff.cav})}{Mean\ (P_{diff.ext} - P_{diff.int})} \tag{3}$$

Where, $P_{diff.ext}$ is the differential external pressure and $P_{diff.int}$ is the differential internal pressure.

Table 2. Comparison of load sharing ratios from experimental data at 0° wind direction and EN 16612

	Closed Cavity			Vented Cavity			EN
	22.4m/s	31.3m/s	40.2m/s	22.4m/s	31.3m/s	40.2m/s	16612
LSR	0.229	0.231	0.258	0.02	~0	~0	0.250

WDR Water Penetration

Wind-driven rain (WDR) tests were performed as indicated in the test protocol in Table 1, on both closed and vented cavity configurations. No water penetration was observed beyond the internal glass wall in both configurations. However, water penetration and mist were observed within the cavity of the vented cavity double skin unit. This indicates that the closed cavity configurations have a better water penetration resistance in comparison to the vented cavity configuration. Accurate manufacturing control is, therefore, necessary also avoid this issue. Figure 13 shows the water penetration observed within the cavity of the vented cavity double skin units. Quantitative measurement of the water in the cavity was impractical given the scale of the tests carried out and the sensitivity of the cavity to openings. However, further studies are recommended to quantify the water penetration in the cavity as this might disrupt the serviceability during the design life, especially because of the inaccessibility of the cavity.

Figure 13. Water penetration in the cavity (Courtesy of WOW Research Team)

CONCLUSION AND RECOMMENDATION

1. As expected, mullions are unaffected by changes in the permeability of double skin units. However, the external and internal glazing are affected by changes in the permeability of the cavity.
2. Higher permeability resulted in larger wind loads on the external glazing in the double skin curtain wall unit. For example, a 78.5mm² increase in opening area, increased the wind load on the external wall by 25% for this test case. This indicates how sensitive the closed cavity load sharing is, to small levels of permeability variations.
3. The load sharing analysis indicates that closed cavity double skin units allow the designer to control which wall carries more loads by varying the permeability. An accurate design strategy, manufacturing control, and durability/aging assessment should be coupled with an optimized load sharing design method to achieve this.
4. Double skin curtain walls are resistant to wind-driven rainwater penetration beyond the internal wall irrespective of cavity permeability for the considered test range. However, permeability influences water penetration into the cavity.

Further studies are recommended using more levels of permeability and different double skin unit parameters (i.e., cavity volume) to better understand the influence of permeability on the performance of double skin curtain walls. Also, it would be important to investigate the way the total opening area is distributed between the two skins and evaluate the impact of this parameter on load sharing.

ACKNOWLEDGEMENT

The experiments were conducted at the NHERI WOW Experimental Facility (National Science Foundation Award No. CMMI 1520853 and No. 2037899). This paper is based upon work sponsored by the US National Science Foundation under the awards NSF IIP1841503 and I/UCRC Wind Hazard and Infrastructure Performance (WHIP) #2020-04. The authors also would like to thank Permasteelisa group for providing the curtainwall sample and installation work. The opinions, findings, conclusions, or recommendations expressed in this paper are solely those of the authors and do not represent the opinions of the funding agencies.

REFERENCES

AAMA (American Architectural Manufacturers Association). 2005. Standard Test Method For Water Penetration Of Windows, Curtain Walls And Doors Using Dynamic Pressure. AAMA 501.1-05. Schaumburg, IL: AAMA.

Baskaran, B. A., and W. C. Brown. 1992. "Performance of Pressure Equalized Rainscreen Walls under Cyclic Loading." *J. Therm. Envel. Build. Sci.*, 16(2), 183–193.

CEN (European Committee on Standardization). 2017. Glass in Building - Determination of the lateral load resistance of glass panes by calculation. EN 16612: 2017. Brussels, Belgium: CEN.

ESDU (Engineering Sciences Data Unit). 2001. Characteristics of the Atmospheric Boundary Wall, Part II: Single Point Data for Strong Winds (Neutral Atmosphere). ESDU Item 85020. London: ESDU.

Fang, Y., S. Memon, J. Peng, M. Tyrer, and T. Ming. 2020. "Solar thermal performance of two innovative configurations of air-vacuum walled triple glazed windows." *Renew. Energy*, 150, 167–175.

Gan Chowdhury, A., I. Zisis, P. Irwin, G. Bitsuamlak, J. P. Pinelli, B. Hajra, and M. Moravej. 2017. "Large-scale experimentation using the 12-fan wall of wind to assess and mitigate hurricane wind and rain impacts on buildings and infrastructure systems." *J. Struct. Eng.*, 143(7).

Ganguli, U., and W. A. Dalgliesh. 1988. "Wind Pressures on Open Rain Screen Walls: Place AIR Canada." *J. Struct. Eng.*, 114(3), 642–656.

Garden, G. K. 1963. *Rain Penetration and its Control. Canadian Building Digest (CBD) Publication 40*. National Research Council Canada.

Kala, S., T. Stathopoulos, and K. Suresh Kumar. 2008. "Wind loads on rainscreen walls: Boundary-wall wind tunnel experiments." *J. Wind Eng. Ind. Aerodyn.*, 96(6–7), 1058–1073.

Killip, I. R., and D. W. Cheetham. 1984. "The prevention of rain penetration through external walls and joints by means of pressure equalization." *Build Environ.*, 19(2), 81–91.

Matthews, R. S., M. R. C. Bury, and D. Redfearn. 1996. "Investigation of dynamic water penetration tests for curtain walling." *J. Wind Eng. Ind. Aerodyn.*, 60(1–3), 1–16.

Mooneghi, A. M., P. Irwin, and A. Gan Chowdhury. 2016. "Partial turbulence simulation method for predicting peak wind loads on small structures and building appurtenances." *J. Wind Eng. Ind. Aerodyn*., 157, 47-62.

Moravej, M. 2018. "Investigating scale effects on analytical methods of predicting peak wind loads on buildings." PhD diss., Florida International University (FIU) Electronic Theses and Dissertations. 3799. https://digitalcommons.fiu.edu/etd/3799.

Suresh Kumar, K. 2000. “Pressure equalization of rainscreen walls: A critical review.” *Build Environ.*, *35*(2), 161–179.

Tokay, A., P. G. Bashor, E. Habib, and T. Kasparis. 2008. Raindrop size distribution measurements in tropical cyclones. Monthly Weather Review, 136(5), pp.1669-1685.

USDOE (US Department of Energy). 2011. *Building energy data book*. Washington, D.C.: USDOE.

Van Linden, S., and N. Van Den Bossche. 2021. Watertightness performance of face-sealed versus drained window-wall interfaces. *Build Environ.*, 196.

Vutukuru, K. S., M. Moravej, A. Elawady, and A. G. Chowdhury. 2020. “Holistic testing to determine quantitative wind-driven rain intrusion for shuttered and impact resistant windows.” *J. Wind Eng. Ind. Aerodyn*., 206, p.104359.

Wu, M. H., T. S. Ng, and M. R. Skitmore. 2016. “Sustainable building envelope design by considering energy cost and occupant satisfaction.” *Energy Sustain Dev.*, 31, 118–129.